phys. stat. sol. (a) **63**, 345 (1981)

Subject classification: 1; 22.1.1

Department of Physics, Erevan State University[1]) *(a) and I. V. Kurchatov Institute of Atomic Energy, Moscow*[2]) *(b)*

The Forbidden-Reflection Method for Absorption Coefficient Measurement in Many-Wave X-Ray Diffraction in Single Crystals

By

R. Ts. GABRIELYAN (a) and V. G. KOHN (b)

A method for the measurement of the effective absorption coefficient for the case of many-wave X-ray diffraction is proposed based on the utilization of a double-block crystal in many-wave configurations, where one of the reflections is being forbidden. Due to the diffraction on the first block (the collimator) a beam corresponding to the forbidden reflection arises. It is truly many-wave and is not accompanied by the non-desired two-wave background. On the base of many-wave scattering dynamic theory, equations are obtained for integrated intensity in a double-block crystal. Quantitative comparison of the theory and experiment is carried out for the case of (111/200) three-wave diffraction of CuK_α radiation in Ge crystal.

Предложен метод измерения эффективного коэффициента поглощения в случае многоволновой дифракции рентгеновских лучей, основанный на использовании двухблочного кристалла и таких многоволновых конфигураций, в которых одно из отражений является запрещенным. В результате дифракции на первом блоке-коллиматоре, возникает пучок, соответствующий запрещенному отражению, который является истинно многоволновым и не сопровождается нежелательным двухволновым фоном. Получены формулы для теоретического расчета интегральной интенсивности в двухблочном кристадле на базе динамической теории многоволнового рассеяния. Проведено конкретное количественное сравнение результатов теории и эксперимента для (111/200) трехволновой дифракции CuK_α излучения в кристалле германия.

1. Introduction

In recent years a number of papers have been published devoted to the theoretical and the experimental investigation of X-ray dynamic many-wave diffraction. Many of them are devoted to one of the most interesting features of this effect, namely to the additional decrease of the absorption coefficient, compared with the two-wave case. The effect was originally revealed by Borrmann and Hartwig [1] and later explained and theoretically analyzed by many authors (see, e.g., [2 to 7]). However, up to date there exists only qualitative coincidence between theory and experiment, which in many cases transforms to a full disagreement. The reason is that the theoretical analysis is traditionally performed in the approximation of a plane incident wave; hence the experimental verification of the theory requires an additional monochromatization of the radiation and a notable decrease of its angular divergency in two directions. This problem is technically a very difficult one, and it is not solved up to date. Additional problems arise from the adjustment of the experimental set

[1]) Mravyan 1, Erevan 49, USSR.
[2]) 123182 Moscow, USSR.

and also from filming due to the weak intensity of X-ray tube radiation. Therefore, in most of experimental works [8 to 11] the many-wave diffraction is observed by filming a conveniently oriented crystal in the "raw" radiation, i.e. in the non-monochromatic and divergent radiation of a sharp focused X-ray tube, meanwhile the diffraction pattern is being fixed on the film.

The theoretical description of the diffraction pattern in the experiments of such a type requires the approximation of a spherical incident wave [12] with corrections, taking account of the radiation non-monochromaticity. However, the theory presented in [12] demands extensive computer calculation, which has not been performed yet.

The measurement and calculation of the integrated intensity of diffracted waves permits to avoid the above-mentioned difficulties and to put successfully into practice the quantitative comparison of theory and experiment. In this case the experimental integrated intensity is determined by means of photometry of many-wave spots on the film, while the theoretical value may be calculated in the approximation of a plane incident wave as an integral over all the incidence angles. An attempt of such a comparison was undertaken in [13, 14]. In [14] the incident beam was monochromatized by Johannson's method, but the angular divergence was $2° \times 2°$. Due to the large angular divergence of the beam the double-wave lines for the reflections of the given configurations are fixed on the film together with the many-wave region. This fact somehow makes the integrated intensity determination difficult. Besides, with such an approach on the base of integrated intensity one can determine only the local (for a given thickness) effective absorption coefficient by means of the results of measurements for two near-by thicknesses.

In the present paper we offer a new method for the measurement of X-ray effective absorption coefficient based on the utilization of a double-block crystal [15] and many-wave configuration, where one of the reflections is forbidden for the two-wave scattering. The first block serves as the collimator, while the second one as the specimen, and is being cut step-like, thus permitting to perform measurements for various thicknesses by simple movement of the crystal (see Fig. 1). The diffracted beam corresponding to the forbidden reflection is excited only in the many-wave angular region and is free from non-desirable double-wave background. Hence, in the process of the diffraction of this beam in the second block, all the diffracted beams appear to be free from double-wave background, thus permitting to perform an absolute measurement of the many-wave integrated intensity. Besides, by setting the film between the blocks, one can measure the intensity of the "incident" radiation and, therefore, determine the integrated effective absorption coefficient (for a given thickness).

The method described was applied to the investigation of (111/200), three-wave diffraction of CuK_α radiation in a Ge crystal. In Section 2 we consider the general theory of many-wave diffraction in a double-block crystal. Experimental methods are

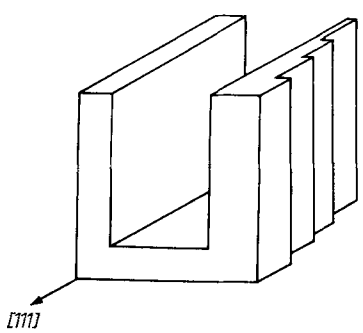

Fig. 1. General view of the two-block crystal

described in Section 3. In Section 4 the experimental results are presented along with their comparison with the theoretical ones.

2. Theory

It is known that in the case of arbitrary incidence upon the crystal the calculation of absorption and transmission coefficients may be performed only by means of numerical computer calculations. The formulation of a many-wave scattering dynamical theory in a form convenient for such a task, is given in [16]. Here we discuss the specific features of many-wave scattering with regard to a double-block crystal.

Consider a wave vector $\boldsymbol{\varkappa}_0$ precisely satisfying the Bragg diffraction condition for a given set of reciprocal lattice vectors $\boldsymbol{h}_m$, i.e.

$$(\boldsymbol{\varkappa}_0 + \boldsymbol{h}_m)^2 = \varkappa_0^2; \qquad |\boldsymbol{\varkappa}_0| = \varkappa = 2\pi/\lambda\,, \tag{1}$$

where λ is the radiation wavelength. The wave vector $\boldsymbol{k}_0$ of the incident wave is more conveniently written in the form

$$\boldsymbol{k}_0 = \boldsymbol{\varkappa}_0 + \boldsymbol{q}; \qquad \boldsymbol{q} = \varkappa(\boldsymbol{e}_{0\pi}\theta_1 + \boldsymbol{e}_{0\sigma}\theta_2)\,. \tag{2}$$

Here $\boldsymbol{e}_{0\pi}$ and $\boldsymbol{e}_{0\sigma}$ are mutually perpendicular unit vectors in the plane normal to $\boldsymbol{\varkappa}_0$. θ_1 and θ_2 determine the angular deviations of incident plane waves from the exact Bragg direction. $\boldsymbol{e}_{0\pi}$ and $\boldsymbol{e}_{0\sigma}$ are simultaneously polarization vectors for the X-ray electric field expansion in the incident and transmitted waves. If the incident wave is polarized in the state s ($s = \pi,\ \sigma$) and its amplitude is A_{0s}, then the electric field amplitude in the m-th diffracted wave after the first block in polarization state m can be written as [17]

$$E_{ms'}(\boldsymbol{r}) = \exp\,[i\boldsymbol{k}_0 \cdot \boldsymbol{r}_1 + i\boldsymbol{k}_m \cdot (\boldsymbol{r} - \boldsymbol{r}_1)]\left(\frac{\gamma_0}{\gamma_m}\right)^{1/2} \boldsymbol{e}_{ms'} P_{m0}^{s's}\,(q, t_0)\, A_{0s}\,. \tag{3}$$

Here $\boldsymbol{r}_1$ is a point on the entrance surface of the first block, t_0 the thickness of the first block, γ_m the cosine of the angle between the normal $\boldsymbol{n}$ to the entrance face and the vector $\boldsymbol{k}_m$,

$$\boldsymbol{k}_m = \boldsymbol{k}_0 + \boldsymbol{h}_m - \alpha_m(q)\,\boldsymbol{n}/2; \qquad \alpha_m = \frac{2\boldsymbol{h}_m\boldsymbol{q}}{\varkappa\gamma_m}\,. \tag{4}$$

$\boldsymbol{e}_{ms}$ are polarization vectors for the m-th diffracted wave. $P_{mn}^{ss'}$ generally is the scattering amplitude from wave (n, s') to wave (m, s),

$$P_{mn}^{ss'}(t) = \sum_j B_{ms'}(j)\, B_{ns'}(j) \exp\,[i(\varepsilon_j + \alpha_m - \alpha_n)\, t/2]\,. \tag{5}$$

Here $B_{ms}(j)$ and ε_j are, respectively, normalized eigenvectors and eigenvalues of the scattering matrix $G_{hk}^{ss'}$,

$$\sum_{ks'} G_{hk}^{ss'} B_{ks'}(j) = \varepsilon_j B_{hs}(j)\,. \tag{6}$$

It can be expressed by the Fourier components of the complex polarizability of the crystal, χ, and in the dipole approximation it may be written as

$$G_{hk}^{ss'} = \frac{\varkappa}{\sqrt{\gamma_h\gamma_k}}\,\chi_{h-k}(e_{hs}e_{ks'}) - \alpha_h\delta_{hk}^{ss'}\,. \tag{7}$$

However, in [16] it is shown that it is sufficient to find the solution of (6) only for its real part G_r, which describes the scattering in a non-absorbing crystal, while the

absorption coefficients $\mu_j = \varepsilon_j''$ ($\varepsilon = \varepsilon' + i\varepsilon''$) can be found as a matrix element of its imaginary part G_i. In this approximation the eigenvectors are orthogonal to one another, i.e.

$$\sum_{ns} B_{ns}(j)\, B_{ns}(j') = \delta_{jj'} . \tag{8}$$

Besides, we have

$$\sum_{j} B_{ns}(j)\, B_{ms'}(j) = \delta_{nm}^{ss'} . \tag{9}$$

Each of the beams diffracted in the first block, automatically appears to be in Bragg direction in the second block, too. It generates once more the whole set of diffracted plane waves with the same wave vectors. The amplitude of the n-th diffracted wave after the second block, originating from the m-th wave after the first block, is given by an expression similar to (3), where the amplitude A_{0s} should be replaced by $E_{ms'}$, and the phase factor should be changed. Finally, after summation over all polarization states, we obtain

$$\boldsymbol{E}_n(m) = \exp\left[i\varphi(r)\right]\left(\frac{\gamma_0}{\gamma_n}\right)^{1/2} \sum_{ss'} \boldsymbol{e}_{ns'} F_{n0}^{s's}(m)\, A_{0s} , \tag{10}$$

where

$$\varphi(\boldsymbol{r}) = \boldsymbol{k}_0 \cdot \boldsymbol{r}_1 + \boldsymbol{k}_m \cdot (\boldsymbol{r}_2 - \boldsymbol{r}_1) + \boldsymbol{k}_n \cdot (\boldsymbol{r} - \boldsymbol{r}_2) , \tag{11}$$

$$F_{n0}^{s's}(m) = \sum_{s''} P_{nm}^{s's''}(t)\, P_{m0}^{s''s}(t_0) . \tag{12}$$

Here t is the varying thickness of the second block.

In the plane wave approximation the phase factor in (10) appears to be non-significant, since the intensity of the diffracted waves in this case does not depend on the coordinates. However, it is significant in the theory of spherical wave diffraction [12, 17], determining the geometrical position of many-wave spots on the film. Since both blocks of the crystal are parallel, the diffraction of the m-th beam in the second block is again described by a matrix of type (7), where one should just change the diagonal elements, namely α_h should be replaced by $\alpha_h - \alpha_m$. The eigenvectors B_{ms} remain unaltered. Finally, in this case, in distinction from Bragg diffraction [17], the scattering amplitudes for both blocks are expressed through the same eigenvectors and eigenvalues.

For a double-block crystal the reflection coefficients of a plane wave are being determined as usually. For non-polarized radiation one has

$$R_n(m) = \frac{\gamma_n}{\gamma_0} \frac{|E_n(m)|^2}{|A_0|^2} = \frac{1}{2} \sum_{ss'} |F_n^{ss'}(m)|^2 , \tag{13}$$

here $|A_0|^2 = |A_{0\pi}|^2 + |A_{0\sigma}|^2$.

Henceforward we shall be interested in the integrated intensity after the second block corresponding to the m-th beam after the first block. It is proportional to

$$\overline{I}_m(t) = \int \mathrm{d}\theta_1\, \mathrm{d}\theta_2\, I_m(t, \theta_1, \theta_2) , \tag{14}$$

where

$$I_m(t, \theta_1, \theta_2) = \sum_{n} R_n(m) = \tfrac{1}{2} \sum_{nss'} |F_n^{ss'}(m)|^2 . \tag{15}$$

Taking into consideration (12), one can rewrite the expression for I_m in a more convenient form

$$I_m(t) = \sum_{s_1 s_2} K_{s_1 s_2}(t_0)\, A_{s_1 s_2}(t)\,, \tag{16}$$

where

$$K_{s_1 s_2}(t_0) = \tfrac{1}{2} \sum_{s} P_{m0}^{s_1 s}(t_0)\, \left(P_{m0}^{s_2 s}(t_0)\right)^*\,, \tag{17}$$

$$A_{s_1 s_2}(t) = \sum_{ns} P_{nm}^{s s_1}(t)\, \left(P_{nm}^{s s_2}(t)\right)^*\,. \tag{18}$$

Note that the matrix $K_{s_1 s_2}(\theta_1, \theta_2)$ in fact acts as a "collimator". If the index m corresponds to a forbidden reflection for a two-wave diffraction, then this function notably differs from zero only in the many-wave angular region, independent of the value of index n. By substituting (5) in (17) one comes to a double sum over the branches of the dispersion surface, i.e. over the indices j and j'. However, the terms with $j \neq j'$ contain factors that rapidly oscillate with varying angles θ_1 and θ_2, hence they give no considerable contribution to the integral (13). By neglecting these terms one obtains

$$K_{s_1 s_2}(t_0) = \tfrac{1}{2} \sum_{j} \mathrm{e}^{-\mu j t_0}\, B_{m s_1}(j)\, B_{m s_2}(j) \sum_{s} B_{0s}^2(j)\,. \tag{19}$$

The expression for $A_{s_1 s_2}$ is obtained in a similar way. (Note that in this case the terms with $j \neq j'$ are exactly zero due to (8).)

$$A_{s_1 s_2}(t) = \sum_{j} \mathrm{e}^{-\mu j t}\, B_{m s_1}(j)\, B_{m s_2}(j)\,. \tag{20}$$

We determine the integrated effective absorption coefficient $\mu_{\mathrm{int}}(t)$ by the following expression:

$$\bar{I}_m(t) = \bar{I}_m(0) \exp\left[-\mu_{\mathrm{int}} t\right]\,. \tag{21}$$

Such a determination permits to obtain the effective absorption coefficient on the basis of a single measurement for one thickness provided the incident intensity is known. Note that the expression for $I_m(0)$ can be simplified by taking into consideration (9),

$$I_m(0) = \sum_{s} K_{ss}(t_0)\,. \tag{22}$$

In [13, 14] the authors considered a local effective absorption coefficient $\mu_{\mathrm{loc}}(t)$, determined as

$$\mu_{\mathrm{loc}}(t) = -\frac{\mathrm{d} \ln\left[\bar{I}(t)\right]}{\mathrm{d}t}\,. \tag{23}$$

In fact, the derivative was replaced by the difference between the values of the function for two close thicknesses.

One can easily show that

$$\mu_{\mathrm{int}} = \frac{1}{t} \int_0^t \mu_{\mathrm{loc}}(t')\, \mathrm{d}t'\,. \tag{24}$$

Since μ_{loc} is monotonously decreasing with increase of t, according to (24) μ_{int} in the whole thickness region prevails over μ_{loc} and tends to its limit more slowly. However,

μ_{int} is more convenient for a comparison between theory and experiment, since in this approach one does not need to calculate the small difference of two close values.

3. Experiment

In many-wave investigations the specimen adjustment is considerably simplified if the crystal is cut in such a way that its horizontal plane is the scattering plane for one of the reflections (e.g. with reciprocal lattice vector $\boldsymbol{h}_1$), i.e. it is the plane containing the incident and the diffracted beam. In this case the crystal is set in a many-wave scattering position by a simple rotation about a vertical axis. If the normal $\boldsymbol{n}$ to the entrance surface of the crystal is normal to $\boldsymbol{h}_1$, then the angle φ between $\boldsymbol{n}$ and the intersection line of reflecting planes is

$$\cos\varphi = \frac{\cos\beta}{\cos\theta_{B1}}. \tag{25}$$

Here β is the angle between the incident beam direction and the intersection line. It is determined by

$$\sin\beta = \frac{R}{\varkappa} = \frac{|\boldsymbol{h}_1 - \boldsymbol{h}_2|}{2\varkappa\sin\alpha} = \\ = \frac{(\sin^2\theta_{B1} + \sin^2\theta_{B2} - 2\sin\theta_{B1}\sin\theta_{B2}\cos\alpha)^{1/2}}{\sin\alpha}, \tag{26}$$

where R is the radius of a circle circumscribed around the polygon of reciprocal lattice vectors, α the angle between $\boldsymbol{h}_1$ and $\boldsymbol{h}_2$, θ_{B1} and θ_{B2} are Bragg angles for the corresponding reflections. Note that in this case we always have $\gamma_0 = \gamma_1 = \cos\theta_{B1}$. Expressions (25) and (26) were the basic ones for the preparation of the specimen.

Our experiment was performed on an A-3 chamber (Japan). Diffraction patterns in a three-wave (111/200) case were filmed for CuK_α radiation diffraction in a Ge crystal. The reflection (200) in Ge is forbidden, hence the corresponding beam originates only in the many-wave angular region and is not accompanied by a two-wave background.

The specimen was prepared in two blocks on a common base (Fig. 1). The lateral surface is (111). In the case under consideration $\varphi = 10°$. Reflection surfaces and the angle φ are presented on Fig. 2. The thickness of the first block was equal to $t_0 = 0.4$ mm, and it serves as a collimator, in order to obtain a nearly parallel "incident" beam for the second block, namely the "forbidden" (200) beam. The second block is step-like with step thicknesses $t = 0.13$, 0.27, 0.46, 0.62 mm. The distance between the blocks is 5 mm, between the source and the crystal 40 cm, and between the crystal and the film 4 cm.

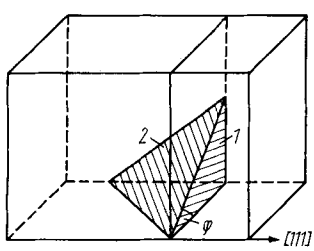

Fig. 2. Geometrical position of reflecting surfaces in the crystal. 1 corresponds to the (111) surface; 2 to the (200) surface

On obtaining a many-wave diffraction in the first block, by means of a scanning mechanism a crystal position can be found in which the second-block diffraction takes place on a step with given thickness. The exposure time was matched in order to have a straight-line region of the densitometer curve. It was from 3 to 20 h, depending on step thickness. The intensity of reflections was measured by a microphotometer MPH-4. In order to determine the incident beam intensity, the film had been set between the interferometer blocks and the intensity of the forbidden beam was measured. Accidental errors connected with thickness measurements were excluded by obtaining several diffraction patterns for various regions of the same thickness and by averaging the results.

4. Results. Comparison of Theory and Experiment

An X-ray pattern obtained with the film between the specimen blocks is presented on Fig. 3. The many-wave regions can be easily seen on all the reflections. However, in the transmitted beam one can see besides the many-wave spots, the double-wave lines as well. These correspond to the double-wave Borrmann effect for the (111) reflection.

Between the crystal blocks all the beams are spatially divided. On the X-ray pattern, as a result, we have nine many-wave regions (see Fig. 4), and four of them have no double-wave background. The integrated blackening of three such regions has been measured (the regions arising after the 200 beam diffraction after the first block), and the effective absorption coefficient was subsequently calculated in accordance with (21).

In order to compare the experimental results with the theory, a computer calculation of the angular dependence of the intensity for diffracted waves was performed on a B CM-6 computer in accordance with (16), (19), (20) for the angular regions

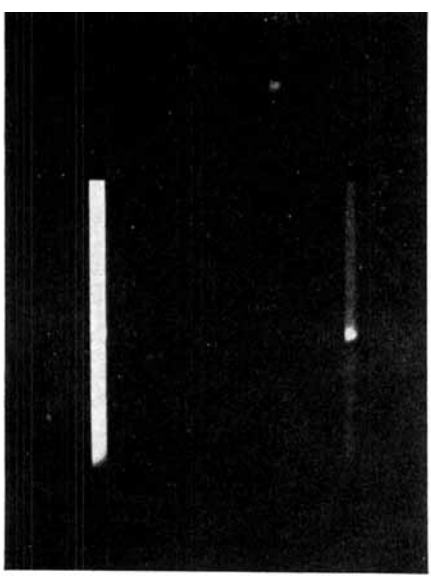

Fig. 3

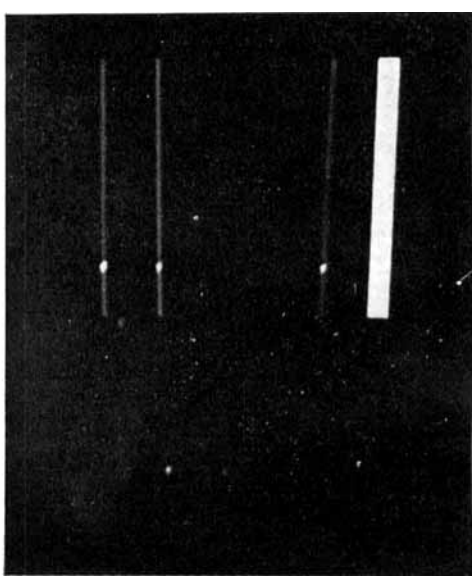

Fig. 4

Fig. 3. X-ray pattern obtained with the film between the blocks

Fig. 4. X-ray pattern after the second block

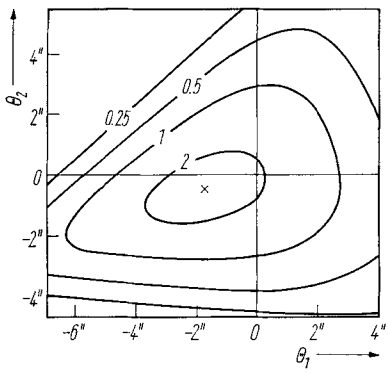

Fig. 5

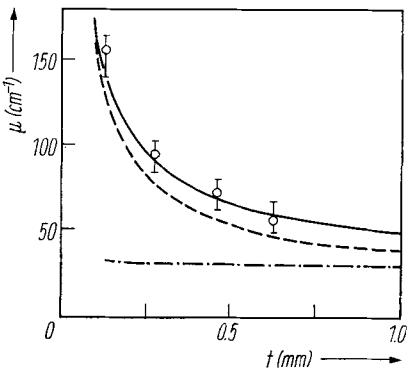

Fig. 6

Fig. 5. Angular dependence of the absorption coefficient for the forbidden (200) reflection after diffraction in first block only. The numbers near the curves are absorption coefficients in per cent

Fig. 6. Theoretical curves for $\mu_{\text{int}}(t)$ (solid line), $\tilde{\mu}_{\text{int}}(t)$ (dashed line), and $\mu_{\overline{\text{loc}}}(t)$ (dash–dotted line) along with experimental values of $\mu_{\text{int}}(t)$

$-7.25'' < \theta_1 < 4.25''$, $-5.75'' < \theta_2 < 5.75''$. The angular dependence of the forbidden reflection after the first block, calculated by (22), is presented on Fig. 5. The vectors $\boldsymbol{e}_{0\pi}$ and $\boldsymbol{e}_{0\sigma}$ in (2) were chosen in such a way that $\boldsymbol{e}_{0\sigma}$ is in the reciprocal lattice vector plane, and the angle included between $\boldsymbol{e}_{0\sigma}$ and $h_2(200)$ is acute; $\boldsymbol{e}_{0\pi} = \boldsymbol{e}_{0\sigma} \times \boldsymbol{s}_0$, where $\boldsymbol{s}_0$ is the unit vector along $\boldsymbol{\varkappa}_0$.

It should be noted that due to radiation non-monochromaticity, the real angular region excited at many-wave diffraction, is noticeably smeared in θ_1-direction [12]. The non-monochromaticity along with final focal dimensions of the X-ray tube lead to a considerable widening of the many-wave region on the X-ray pattern. However, this is not essential when calculating the effective absorption coefficient via the integrated intensity, since the factors describing the widening do not depend on the crystal thickness.

The calculated dependence of $\mu_{\text{int}}(t)$ and the experimental values for four thicknesses are presented on Fig. 6. The disagreement between experimental and theoretical values is small and is in the limits of error of the intensity measurement by the microphotometer. It should be mentioned that a reasonable agreement between theoretical and experimental results is obtained for all the thicknesses including very small ones ($t \approx 0.1$ mm), while in [14] the coincidence between theory and experiment was obtained only for $t > 1$ mm.

On Fig. 6 the dependence of $\tilde{\mu}_{\text{int}}(t)$ calculated from the intensity values in exact Bragg position, and $\mu_{\text{loc}}(t)$ are shown for comparison. One can see that in the case of small thicknesses the role of angular divergence appears to be non-essential when calculating μ_{int}. The explanation of this fact is that at small thicknesses the integrated intensity is contributed by all the Bloch waves, including those with large absorption coefficients. The intensity of such waves increases along with the deviation from the Bragg direction, thus compensating the intensity decrease for anomalously transmitted waves. The increase of thickness results in an imbalance, and the difference between μ_{int} and $\tilde{\mu}_{\text{int}}$ becomes noteciable.

The obtained results permit to conclude that the method of the forbidden reflection is a relatively simple and effective one for quantitative measurements in X-ray many-wave scattering and for a successful experimental verification of the many-wave scattering dynamic theory.

References

[1] G. Borrmann and W. Hartwig, Z. Krist. **121**, 401 (1965).
[2] Y. Heno and P. P. Ewald, Acta cryst. **A24**, 16 (1968).
[3] P. Penning, Philips Res. Rep. **23**, 12 (1968).
[4] G. Hildebrandt, phys. stat. sol. **24**, 245 (1967).
[5] T. Joko and A. Fukuhara, J. Phys. Soc. Japan **22**, 597 (1967).
[6] A. M. Afanasev and V. G. Kohn, phys. stat. sol. (a) **28**, 61 (1975).
[7] A. M. Afanasev and V. G. Kohn, Acta cryst. **A33**, 178 (1977).
[8] S. Balter, R. Feldman, and B. Post, Phys. Rev. Letters **27**, 307 (1971).
[9] I. P. Mihalyuk, V. D. Kozmik, S. A. Kshevetskii, and M. B. Ostapovich, Ukr. fiz. Zh. **22**, 224 (1977).
[10] I. P. Mihalyuk, S. A. Kshevetskii, and M. B. Ostapovich, Kristallografiya **23**, 403 (1978).
[11] T. I. Borodina, V. I. Iveronova, A. A. Katsnelson, and T. K. Runova, phys. stat. sol. (a) **28**, 365 (1975).
[12] V. G. Kohn, Fiz. tverd. Tela **19**, 3567 (1977).
[13] W. Uebach and G. Hildebrandt, Z. Krist. **129**, 1 (1969).
[14] W. Uebach, Z. Naturf. **28a**, 1214 (1973).
[15] R. Ts. Gabrielyan, P. A. Bezirganyan, and F. O. Eiramdyan, Kristallografiya **21**, 1190 (1976).
[16] V. G. Kohn, Fiz. tverd. Tela **18**, 2538 (1976).
[17] V. G. Kohn, phys. stat. sol. (a) **54**, 375 (1979).

(Received July 2, 1980)